

A Carrier Communication Channel Modeling Of Marine Electromagnetic Exploration System Based On Multi Conductor Transmission Line Theory

Xiguo Ren¹, Yiming Zhang¹, Haijun Tao^{1,2}, Zhihui Zeng² and Jianzhi Ding¹

¹Beijing University of Technology, Beijing 100124 China; ²Henan Polytechnic University, Jiaozuo 454003 China

xiaoxifree@126.com; ymzhang@bjut.edu.cn; taohj99@hpu.edu.cn;
djzh5@163.com; zzhh@hpu.edu.cn

Abstract

Subsea communication system is a key component of marine electromagnetic exploration system. In subsea communication system, only the power line channel model is fully studied, it could help to achieve high-speed and reliable power line carrier communication. In this paper, a channel model is established by using the theory of multi conductor transmission. The single Pi structure, double Pi structure and T structure cable model have been simulated through the Spice. The accuracy of single Pi structure model was verified by measurement and simulation. It provides a guiding role for the whole communication system.

Keywords: *Marine electromagnetic exploration system; the theory of multi conductor transmission; transmission line model; Spice; the single Pi structure*

1. Introduction

Power line carrier communication (PLC) is a kind of communication mode that carries on the voice or data transmission by the power line as the information transmission medium [1]. Power lines are widely used in thousands of households, and it is widely and economy used as a communication medium. People have a long history of research on power carrier communication technology. And it was applied to the 10 kV distribution network line communications as long as in 1920s. With the rapid development and the rising demand for a variety of communications, power line carrier communication has become a hot research topic in the domestic and foreign researchers [2]. Subsea communication system is a key component of marine electromagnetic exploration system. In subsea communication system, the whole communication system is constituted by the sending / receiving device and a communication channel between them, which transport the data of subsea depth, temperature, output voltage, output current, and emission frequency and so on. The communication channel is a key factor affecting the communication quality of the communication system. Because it is directly related to the signal attenuation, impedance and noise, and there is a very large impact on the transmission and reception. In the marine electromagnetic exploration system, a large number of power electronic devices are used. It presents new problems and challenges to the research of the component impedance model. Therefore, this paper mainly focuses on the research of the subsea communication channel.

In subsea communication system, only the power line channel model is fully studied, it could help to achieve high-speed and reliable power line carrier communication. In recent years, the scholars have a lot of research on the attenuation, impedance and noise of power line. In literature [3], a channel model is established and validated the laboratory simulation circuit based on two-conductor transmission line. In literature [4], a

distribution network power line communication channel model is built based on the node admittance matrix. The test frequency is limited to 120 kHz or less. In literature [5], the attenuation model of low-voltage lines is established based on two-conductor transmission lines and port network theory. While only a small number of scholars have carried out a simple study on the PLC system in the control system of subsea production. In literature [6], there is a brief introduction on the principle of subsea PLC, the structure and modulation. And literature [7] introduces several major modulation schemes. Literature [8-10] gives the design method of subsea wave communication router. But these documents simply introduce the working principle of the communication system, the composition of the modulation and demodulation equipment device [11]. The design and analysis of the actual communication system are rarely involved. Overall, the current research into the model is not directed at the marine electromagnetic exploration system. The model of transmission line has not yet been deeply studied for marine electromagnetic exploration system.

The transmission line of the marine electromagnetic exploration system is usually more than a few kilometers, and the high frequency communication signal is difficult to be described by the top-down method. In this paper, a channel model is established by using the bottom up method. The model parameters are obtained from the bottom up method through theoretical calculation, which has good generality and flexibility, and could well describe the relationship between the channel characteristics and the model parameters. The impedance model of the Towing cable is determined through field measurements based on the impedance measurement. The correctness of the model is verified by experiments. The transmission law of the marine PLC signal would be further study by this model.

2. Synopsis of Marine Electromagnetic Marine Communication System

The marine electromagnetic exploration system adopts subsea system back to platform above water. It is divided into four parts: maritime control section, maritime supply section, Towing cables and subsea electromagnetic marine section. Its structure diagram is shown in Figure 1.

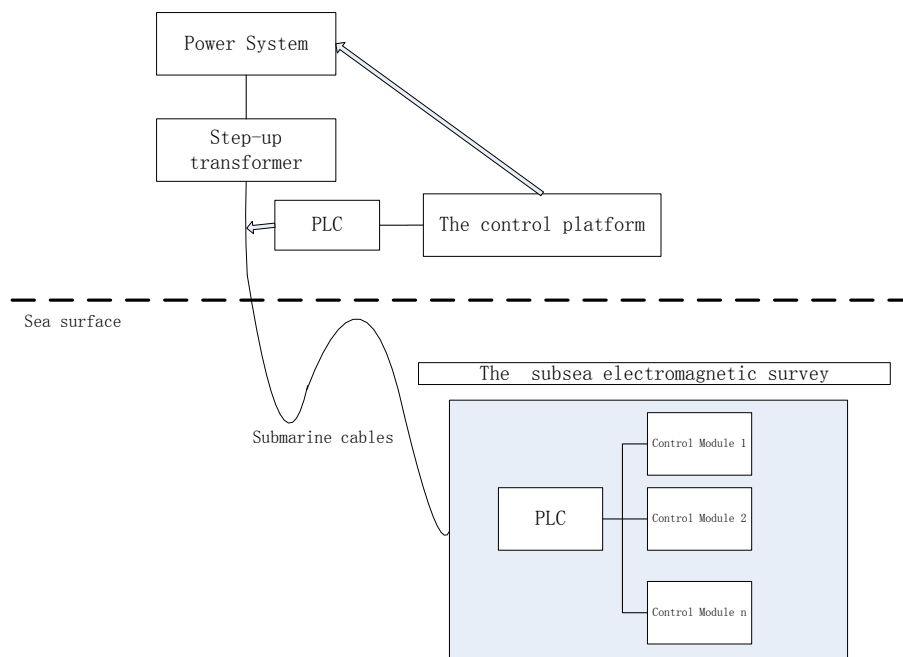


Figure 1. The Structure Diagram of the Marine Electromagnetic Exploration System

From the Figure 1, the maritime carrier equipment is located in the control platform, connected to the towing cables. And the subsea carrier equipment located in the electromagnetic marine section. The power / signal transmission of whole system is connected by a several thousand meters towing cable. Because the control modules of the electromagnetic marine section transmit the signal by the internal signal line, and the carrier signals cannot be transmitted across the transformer. The communication channel of the PLC communication is the terminal of the maritime towing cable to the terminal of the subsea towing cable. In order to achieve high-speed and reliable power line communications, it is necessary to have a good understanding of the power line channel model. Therefore, the main purpose of this paper is to establish the channel model of marine electromagnetic communication.

3. Parameter Calculation of Unit Length Transmission Line in Marine Electromagnetic Exploration System

Since the transmission line uses the coaxial cable in the marine electromagnetic exploration system. The unit length parameter matrix is R, L, G, C. The distribution conductivity of the transmission line is simulated in literature [12]. And its result shows that the electrical conductivity of the e transmission line could be neglected in the range of 30MHz ~ 1Hz. In the marine electromagnetic exploration system the voltage of the towing cable is 3-5KV. Because of the high frequency of power line communication, the skin effect of wire could not be ignored.

Internal to the conductor, the conduction current dominates the displacement current. Therefore, current distribution in the cable conductor could be described by the transmission equation of the transmission line. Assuming that the current density is in the z direction (along the axis of the wire) and on the symmetry of the wire. It is assumed that the current density is independent of z and is a function of the wire radius r. The conduction equation could be described as.

$$\frac{d^2 J_z}{dr^2} + \frac{1}{r} \frac{d J_z}{dr} + k^2 J_z = 0 \quad (1)$$

Here

$$k^2 = -j\omega\mu\sigma = -j\frac{2}{\delta^2} \quad (2)$$

μ is the magnetic permeability of the cable, σ is the electrical conductivity of the cable, δ is the skin depth of the cable, J_z is the current density at the radius r.

The solution to this equation is

$$J_z = J_o \frac{\text{ber}\left(\sqrt{2r/\delta}\right) + j\text{bei}\left(\sqrt{2r/\delta}\right)}{\text{ber}\left(\sqrt{2r_0/\delta}\right) + j\text{bei}\left(\sqrt{2r_0/\delta}\right)} \quad (3)$$

Where $\text{ber}(x)$ and $\text{bei}(x)$ are the real and imaginary parts of the first class deputy variable Bessel function. J_o is the current density of wire outer radius at $r=r_0$.

According to Faraday's law of electromagnetic induction, the magnetic field can be obtained by the product of the conductivity of the conducting cable.

$$\nabla \times \vec{J} = -j\omega\mu\sigma\vec{H} \quad (4)$$

The current density is only related to the radius r in the Z direction. So

$$\frac{dJ_z}{dr} = j\omega\mu\sigma\hat{H}_\phi \quad (5)$$

Substituting (5) into formula (3) gives the calculation formula of the total impedance and the inner inductance (unit length) of the conductor:

$$\frac{R}{R_{dc}} = \frac{q}{2} \left[\frac{\text{ber}\left(\sqrt{2r_w/\delta}\right) \text{bei}'\left(\sqrt{2r_w/\delta}\right) - \text{bei}(q) \text{ber}'\left(\sqrt{2r_w/\delta}\right)}{\left(\text{bei}'\left(q \sqrt{2r_w/\delta}\right)\right)^2 + \left(\text{ber}'\left(\sqrt{2r_w/\delta} q\right)\right)^2} \right] \quad (6)$$

$$\frac{L_i}{L_{i,dc}} = \frac{q}{4} \left[\frac{\text{bei}\left(\sqrt{2r_w/\delta} q\right) \text{bei}'\left(\sqrt{2r_w/\delta}\right) - \text{ber}(q) \text{ber}'\left(\sqrt{2r_w/\delta} q\right)}{\left(\text{bei}'\left(\sqrt{2r_w/\delta}\right)\right)^2 + \left(\text{ber}'\left(\sqrt{2r_w/\delta}\right)\right)^2} \right] \quad (7)$$

Where

$$R_{dc} = \frac{1}{\sigma \pi r_0^2} (\Omega / m) \quad (8)$$

$$L_{i,dc} = \frac{\mu_0}{8\pi} = 0.5 \times 10^{-7} (\text{H} / m) \quad (9)$$

$$\text{bei}'\left(\sqrt{2r_0/\delta}\right) = \frac{d}{dr} \text{bei}\left(\sqrt{2r_0/\delta}\right) \quad (10)$$

$$\text{ber}'\left(\sqrt{2r_0/\delta}\right) = \frac{d}{dr} \text{ber}\left(\sqrt{2r_0/\delta}\right) \quad (11)$$

Since the pilot carrier frequency is generally from tens Hz to hundreds MHz, the unit length of the total impedance and the inner inductance can be simplified as

$$R = \frac{1}{2r_0} \sqrt{\frac{\mu}{\pi\sigma}} \sqrt{f} (\Omega / m) \quad (12)$$

$$L_i = \frac{1}{4\pi r_0} \sqrt{\frac{\mu}{\pi\sigma}} \sqrt{f} (\text{H} / m) \quad (13)$$

4. Towing Cable Model based on Multi Conductor Transmission Line

The series impedance matrix of the towing cable is $Z_0 = R_0 + j\omega L_0$, and its shunt admittance matrix is $Y_0 = j\omega C_0$. Because the outermost shell of the towing cable is the shield shell, The diagonal element Z_{ii} of the Z_0 is the self-impedance impedance of the conductor to the shield for the unit length and diagonal element Z_{ik} is the mutual impedance between the inner and outer conductors^[13].

The simplified formulas for calculating the self-impedance and mutual impedance are such as formula (14) and (15).

$$Z_{ii} = R_{\text{internal}} + j \left(\omega \frac{\mu_0}{2\pi} \ln \frac{2(d_i + p)}{r_i} + X_{\text{internal}} \right) \quad (14)$$

$$Z_{ik} = Z_{ki} = j\omega \frac{\mu_0}{2\pi} \ln \frac{\sqrt{(d_i + d_k + 2p)^2 + x_{ik}^2}}{d_{ik}} \quad (15)$$

Where μ_0 is the permeability, d_i and d_k are respectively the distance of inner and outer conductors to the shield shell, d_{ik} is the distance between the conductors, $p = \sqrt{\rho / j\omega\mu_0}$, r_i is the radius of the wire.

Based on the multi conductor transmission line theory, the transmission line equation of dx length element can be written as

$$\begin{cases} \frac{d}{dz} V(z) = -ZI(z) \\ \frac{d}{dz} I(z) = -YU(z) \end{cases} \quad (16)$$

It is converted into second-order decoupled ordinary differential equations.

$$\begin{cases} \frac{d^2}{dz^2} V(z) = ZYV(z) \\ \frac{d^2}{dz^2} I(z) = YZI(z) \end{cases} \quad (17)$$

In general, ZY and YZ are not diagonal matrices, so the equations could not be solved directly. Mode theory is used to decouple the equation by the voltage conversion matrix T_V and the current transition matrix T_I . The voltage and current of each model is equal to the wave equation of the independent homogeneous system. And they are independent of each other. Hence the transmission line equation can be written as

$$\begin{cases} V(z) = T_V V_m(z) \\ I(z) = T_I I_m(z) \end{cases} \quad (18)$$

Where $V_m(z)$, $I_m(z)$ are column vectors of the mode voltage and the mode current. Therefore, the formula (17) is converted to

$$\begin{cases} \frac{d^2}{dz^2} V_m(z) = T_V^{-1} ZY T_V V_m(z) = \gamma^2 V_m(z) \\ \frac{d^2}{dz^2} I_m(z) = T_I^{-1} YZ T_I I_m(z) = \gamma^2 I_m(z) \end{cases} \quad (19)$$

Because of $T_I^t = T_V^{-1}$,

$$T_V^{-1} ZY T_V = T_I^{-1} YZ T_I = \begin{bmatrix} \gamma_1^2 & \cdots & 0 \\ \vdots & \ddots & \vdots \\ 0 & \cdots & \gamma_n^2 \end{bmatrix} \quad (20)$$

Where $\gamma_i^2 (i=1,2,\dots,n)$ is the characteristic value of ZY and YZ. The towing cable is considered as a 2n port network, and the voltage and current at the distance l from the transmitting terminal are as follows:

$$\begin{bmatrix} U(1) \\ I(1) \end{bmatrix} = \begin{bmatrix} A_{11} & A_{12} \\ A_{21} & A_{22} \end{bmatrix} \begin{bmatrix} U(0) \\ I(0) \end{bmatrix} \quad (21)$$

Where U (1) and I (1) are the voltage vector and current vector at the l, U (0) and I (0) are the voltage vector and current vector at the transmitting terminal. The entire towing cable in accordance with the length of L is divided into N parts. If the length of each section can be seen as electrically short for the frequency, that is

$$\frac{l}{N} \ll \lambda = \frac{v}{f} \quad (22)$$

So each part can be used to characterize the lumped model. As the frequency increases the transmission lines must be divided more finely. The 4 parameters of the Pi structure and the T structure of the lumped model are as follows.

$$A_{pi} = \begin{bmatrix} A_{11} & A_{12} \\ A_{21} & A_{22} \end{bmatrix} = \begin{bmatrix} \left\{ 1_n + \frac{1}{2} \hat{Z} \hat{Y} \left(\frac{1}{N} \right)^2 \right\} & \left\{ -Z \frac{1}{N} \right\} \\ \left\{ -\hat{Y} \frac{1}{N} - \frac{1}{4} \hat{Y} \hat{Z} \hat{Y} \left(\frac{1}{N} \right)^3 \right\} & \left\{ 1_n + \frac{1}{2} \hat{Y} \hat{Z} \left(\frac{1}{N} \right)^2 \right\} \end{bmatrix} \quad (23)$$

$$A_T = \begin{bmatrix} A_{11} & A_{12} \\ A_{21} & A_{22} \end{bmatrix} = \begin{bmatrix} \left\{ 1_n + \frac{1}{2} \hat{Z} \hat{Y} \left(\frac{1}{N} \right)^2 \right\} & \left\{ -\hat{Z} \frac{1}{N} - \frac{1}{4} \hat{Z} \hat{Y} \hat{Z} \left(\frac{1}{N} \right)^3 \right\} \\ \left\{ -Y \frac{1}{N} \right\} & \left\{ 1_n + \frac{1}{2} \hat{Y} \hat{Z} \left(\frac{1}{N} \right)^2 \right\} \end{bmatrix} \quad (24)$$

The \hat{Z} is the unit impedance matrix of towing cable, and the \hat{Y} is the unit admittance matrix of towing cable.

5. Simulations

This paper uses the Cadence/PSPICE software to build the simulation model of the single Pi structure, double Pi structure and T structure as shown in Figure 2-4.

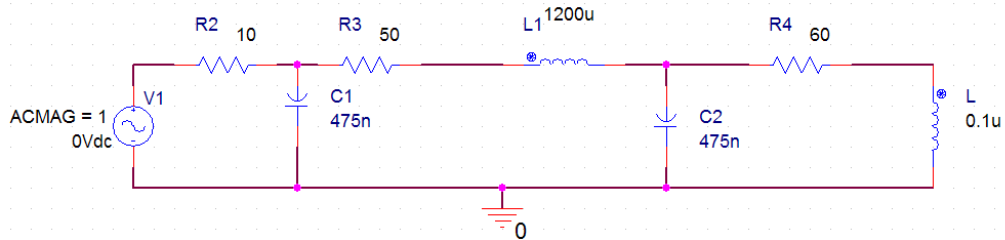


Figure 2. The Model of the Single Pi Structure

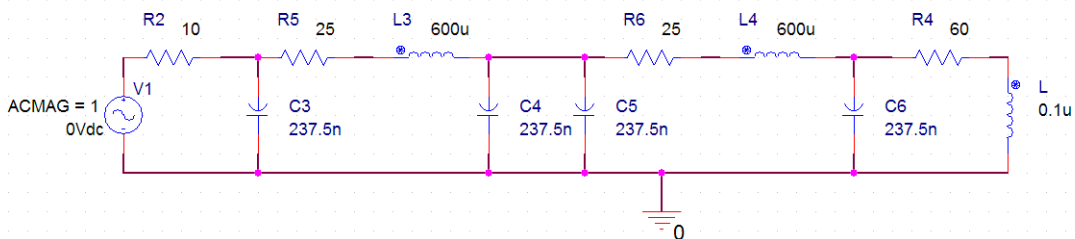


Figure 3. The Model of the Double Pi Structure

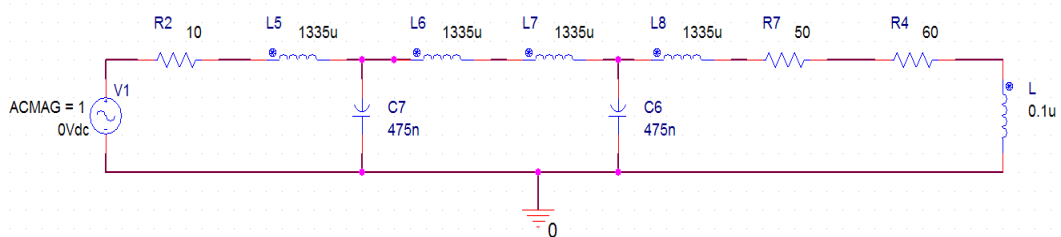


Figure 4. The Model of the T Structure

In the simulation setting, the AC small signal and noise analysis models is selected. Signal source V1 is set to 81dBm, the amplitude is 1, and the phase is 0. In order to obtain the 81dBm transmission power for V1, its internal resistance as 10 ohms. Carrier frequency is from 100Hz to 1MHz. Among the structure, units of the resistance R, inductance L and capacitance C are respectively as the international unit Ω , H and F. The receiver is located in the marine electromagnetic exploration system under water about 10km; the internal resistance is 60 ohm /0.1uH. The simulation results are as follows.

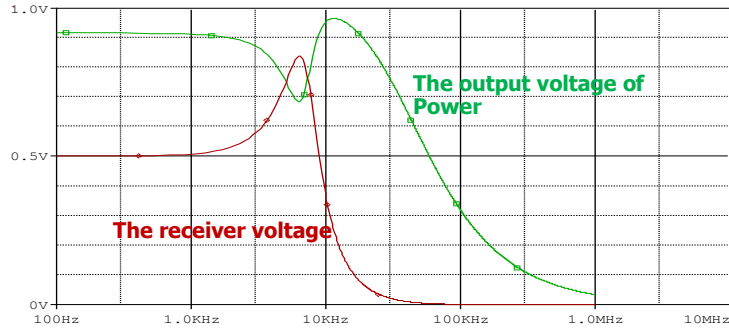


Figure 5. The Simulation Result of the Single Pi Structure

The figure shows the simulation results for the single Pi structure. The power supply voltage drops rapidly but the receiver voltage rises rapidly after the first inflection point which is at 3.5 kHz. And when the frequency is 6.5 kHz, the power supply voltage is reduced to a minimum but the receiver voltage rises to maximum. However, the receiver voltage is greater than the supply voltage from 5.0 kHz to 7.3 kHz, which could not communicate. When the frequency is 13 kHz, there is second inflection point. At this time the receiver can receive the minimum voltage but the power supply voltage rises to maximum. Then the frequency exceeds 16 kHz, both the power supply voltage and the receiver voltage are rapidly fading. The power supply has been unable to output after 30 kHz.

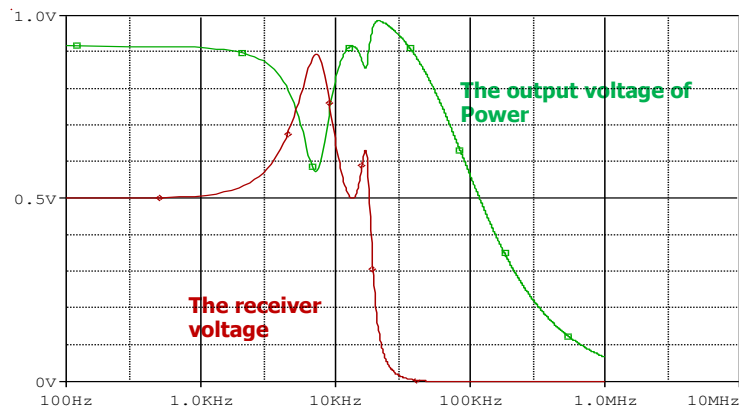


Figure 6. The Simulation Result of the Double Pi Structure

The figure shows the simulation results for the double Pi structure. Like the single Pi structure, the power supply voltage drops rapidly after the first inflection point which is at 4 kHz. And when the frequency is 7 kHz, the power supply voltage is reduced to a minimum but the maximum for the receiver. However, the receiver voltage is greater than the supply voltage from 5.0 kHz to 9.0 kHz, which could not communicate. When the frequency is 13 kHz, there is second inflection point. At this time the receiver could get the minimum voltage but the maximum for the power supply. However, different from the single Pi structure is that when the frequency is 16 kHz, there is third inflection point. At this point, the receiver voltage reaches the peak value again, and the power supply voltage reaches the minimum value. Then the frequency exceeds 16 kHz, the receiver voltage decays rapidly. At last the power supply has been unable to output after 30 kHz.

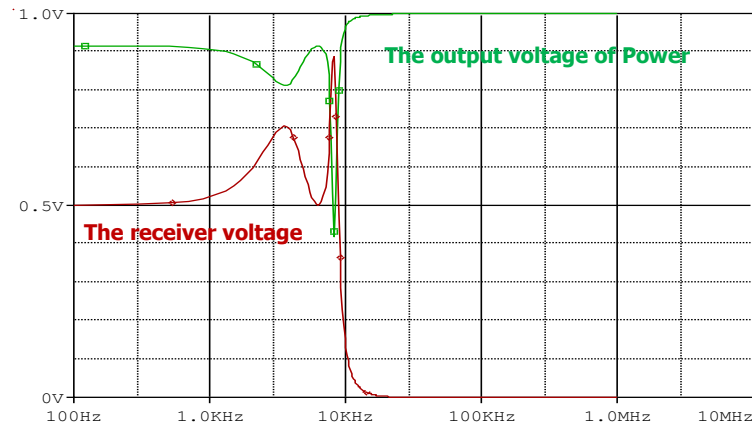


Figure 7. The Simulation Result of the T Structure

The figure shows the simulation results for the double T structure. It is different from the single Pi structure and the double Pi structure. The power supply voltage drops rapidly but the receiver voltage rises after the first inflection point which is at 4 kHz. And when the frequency is 6.5 kHz, the power supply voltage is reduced to a minimum but the maximum for the receiver. There is third inflection point at 8.3 kHz, where the power supply voltage is reduced to a minimum but the maximum for the receiver. After this frequency the receiver voltage decays rapidly. At last the power supply has been unable to output after 15 kHz. However, the receiver voltage is greater than the supply voltage from 7.7 kHz to 8.6 kHz, which could not communicate.

The actual measurement of the T structure could not accurately reflect the actual working mode of the channel, and the double PI structure is a large amount of calculation. Therefore, the single Pi structure is confirmed.

The transmitted signal is 81dB (25W). Meanwhile, the minimum power of the receiver must be greater than or equal to -100 dB (The signal will be lost in the background noise below this value). The receiving signal power could be calculated by the following formula.

$$P_{N*1} = 10 \cdot \lg(I_{N*1} \cdot V_{N*1}) \cdot 1000 \quad (25)$$

Wherein $P_{(N*1)}$ is the receiver signal power. So the receiver signal power of the 3 structures is obtained.

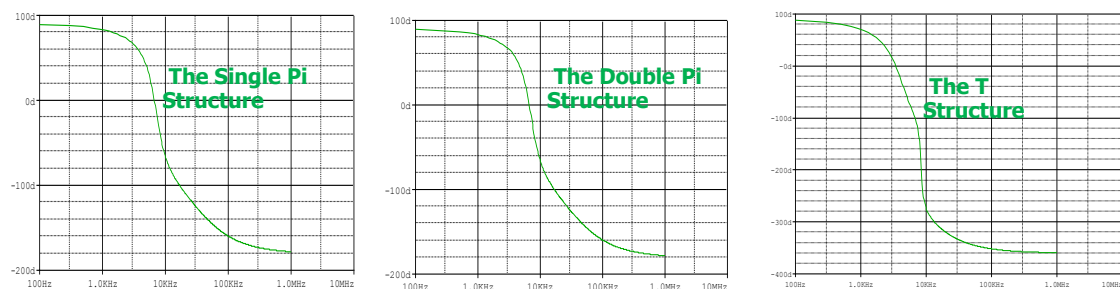


Figure 8: The Curves of the 3 Structures

From the above curves, the receiving signal curve of the single Pi structure is basically consistent with the double Pi structure, but it is larger different with the curve of the T structure. T-type structure has rapidly decay power at 3 kHz. And the receiver could not get the signal after 6.5 kHz. Nevertheless, the power can basically keep consistent around 3 kHz for the single Pi structure and the double Pi structure. The receiver basically could not receive the signal until 13 kHz.

6. Experimental

In this experiment, the inner conductor of towing cable is used AWG1 line (19*0.945), which consists of 19 shares copper wire with 0.945mm diameter. And the outer conductor uses AWG20 line with 1 shells of 0.813mm diameter. The structure of the towing cable is shown in Figure 9 and Table 1.

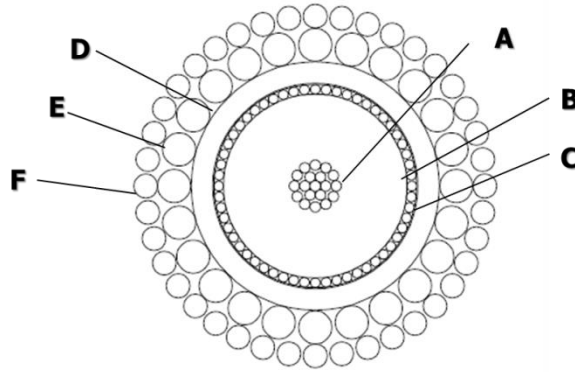


Figure 9. The Structure of the Towing Cable

Table 1. The Parameters of the Towing Cable

Number	Description	D(mm)
A	AWG1	3
B	INSULATION	10.72
C	AWG20	11.86
D	BELT	14.48
E	ARMOR/ Shell 1	18.39
F	ARMOR/ Shell 2	21.20

The distribution resistance, inductance and capacitance of the 10km towing cable are tested using the LCR instrument as shown in the following table. Among them, 0.2, 0.5, 1 and 10km are the measured values, and the other is the theoretical calculation.

Table 2. The Measured Values of RLC

Length/km	R/ Ω	L/ μ H	C/nF
0.2	1.00	24.00	19.00
0.5	2.52	60.20	48.50
0.8	4.90	121.80	96.00
1	4.99	120.35	96.80
2	12.25	304.50	240.00
5	24.50	609.00	480.00
10	50.00	1200.00	950.00

From the above table, the result could be seen that the measured values are in agreement with the theoretical calculation, and there is no big discrepancy between them.

Used digital oscillator and digital frequency selective meter measures the voltage of the receiver. The power supply voltage is 1V (81db), transmit and receive impedance is 50 ohms. Curve fitting of measurement and simulation structure using MATLAB, its result are shown in Figure 10.

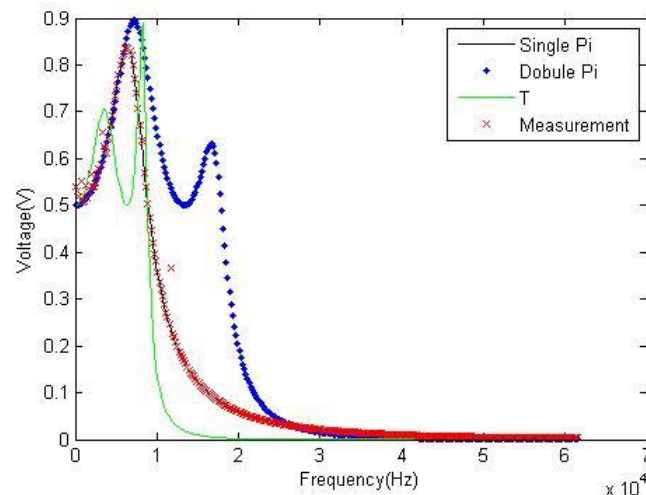


Figure 10: Comparison of Simulation and Measurement Results for Receiver Voltage

It can be seen from the figure that the single Pi structure measurement of the receiver voltage is in agreement with the simulated voltage value. It is only different in low frequency, but this does not affect the analysis of the actual communication.

7. Conclusions

A carrier communication channel model of marine electromagnetic exploration system based on multi conductor transmission line is established in this paper. The basic impedance value of towing cable is obtained by impedance measurement. The single Pi structure, double Pi structure and T structure cable simulation model have been set up through the Spice. The accuracy of single Pi structure model was verified by measurement and simulation. The parameters of this model are easy to be calculated and measured. Accordingly the model could be used to analyze the design of the communication frequency band and the coupling circuit in order to facilitate the application of different modulation and coding technology in marine electromagnetic exploration. It provides a guiding role for the whole communication system.

Acknowledgements

Authors wishing to acknowledge assistance or encouragement from colleagues, financial support by R&D of Key Instruments and Technologies for Deep Resources Prospecting (the National R&D Projects for Key Scientific Instruments), Grant No. XDB06030200.

References

- [1] F. Chen, W. Zheng and C. Sheng, "Low-voltage power line carrier communication technology and its application", *Power System Protection and Control*, vol. 188, no. 22, (2009).
- [2] S. Siami, C. Joubert and C. Glaize, "High frequency model for power electronics capacitors", *IEEE Transactions on Power Electronics*, vol. 157, no. 16, (2001).
- [3] C. Wei, L. Jian and L. Kaipei, "A channel modeling technology for the medium-voltage power-line carrier in smart power distribution grid", *Proceedings of the CSEE*.150, vol. 32, (2012).
- [4] B. Caldon, "Distribution line carrier: analysis procedure and applications to DG", *IEEE Transactions on Power Delivery*, vol. 575, no. 22, (2007).
- [5] S. Galli, T. A. Banwell, "novel approach to the modeling of the indoor power line channel, part II:transfer function and its properties", *IEEE Transactions on Power Delivery*.3, 20, (2005).
- [6] F. Su, H. Liu and Q.Wang, "Application of power / signal transmission technology in underwater production system", *Petrochemical Automation*, vol. 5, no. 29, (2008).

- [7] L. Zhang, "Design of subsea production control systems", Shipbuilding of china, vol. 1, no. 51, (2010).
- [8] H. Shorten V, Stein V. Power line communication device for subsea well. U.S. Patent, vol. 8, no.052, 940, (2010).
- [9] V. Horten and V. Steigen, "Modem in particular for subsea power line communication. U.S. Patent 8, vol. 279, no. 614, (2012).
- [10] E. Brekke, V. Horten and V. Steigen, "Method and modem for subsea power line communication [P]. U.S. Patent 8, vol. 199, no. 798, (2012).
- [11] S. Wang, Y. Liu, H. Cao, L. Guo, Y. Wang, L. Zhu and J. Tian, "Simulation study on power line carrier communication design for subsea production control system", Ocean engineering equipment and technology, vol. 2, no. 64, (2015).
- [12] J. Anatory, N. Theethayi and R. Thottappillil, "Power-line communication channel model for interconnected networks, part II :multi conductor system", IEEE Transactions on Power Delivery, vol. 24, no. 124, (2009).
- [13] H. W. Dommel, "EMTP theory book", USA: Bonneville Power Administration, Columbia, (1986).

Authors



Ren Xiguo , he is from Hebei, China, Beijing University of Technology, PhD, scientific interest: Power electronic, Communications technology, switching supply. E-mail: xiaoxifree@126.com



Zhang Yiming, he is from, Hubei, china, Beijing University of Technology, Professor, PhD, scientific interest: intelligent power management, motor speed control, servo drives, and motor energy conservation. E-mail: ymzhang@bjut.edu.cn



Tao Haijun , he is from, Henan, China, Beijing University of Technology, and PhD, taught at the University of Henan Polytechnic University, Lecturer, and scientific interest: Power electronic, Communications technology, switching supply. E-mail: taohj99@hpu.edu.cn



Zeng Zhihui, he is from Jiangxi, China, University of Henan Polytechnic University, associate professor, PhD, scientific interest: signal processing, Power electronic, Communications technology, Energy storage technology. E-mail: zzhh@hpu.edu.cn



Ding Jianzhi, he is from Liaoning, China, Beijing University of Technology, PhD, scientific interest: High frequency power conversion, geophysical prospecting converter, switching supply. E-mail: djzh5@163.com

